

Reaction of Laser-Ablated Uranium Atoms with CO: Infrared Spectra of the CUO, CUO⁻, OUCCO, (η^2 -C₂)UO₂, and U(CO)_x (x = 1–6) Molecules in Solid Neon

Mingfei Zhou,[†] Lester Andrews,^{*,†} Jun Li,[‡] and Bruce E. Bursten^{*,‡}

Contribution from the Departments of Chemistry, University of Virginia, Charlottesville, Virginia 22901, and The Ohio State University, Columbus, Ohio 43210

Received June 22, 1999

Abstract: Laser-ablated uranium atoms have been reacted with CO molecules during condensation with neon at 4 K. Absorptions at 1047.3 and 872.2 cm⁻¹ are assigned to the CUO molecule formed from the insertion reaction that requires activation energy. Isotopic substitution shows that the upper band is largely U–C and the lower band mostly U–O in vibrational character. Absorptions at 2051.5, 1361.8, and 841.0 cm⁻¹ are assigned to the OUCCO molecule, which is formed by the CO addition reaction to CUO and ultraviolet–visible photon-induced rearrangement of the U(CO)₂ molecule. The OUCCO molecule undergoes further photochemical rearrangement to the (C₂)UO₂ molecule, which is characterized by symmetric and antisymmetric O–U–O stretching vibrations at 843.2 and 922.1 cm⁻¹. The uranium carbonyls U(CO)_x (x = 1–6) are produced on deposition or on annealing. Evidence is also presented for the CUO⁻ anion and U(CO)_x⁻ (x = 1–5) anions, which are formed by electron capture. Relativistic density functional theoretical calculations have been performed for the aforementioned species, which lend strong support to the experimental assignments of the infrared spectra. It is predicted that CUO is a linear singlet molecule with the shortest U–C bond yet characterized, and it has a U–C triple bond with substantial U 5f character. The theoretical analysis also finds that a distorted tetrahedral geometry of (C₂)UO₂ lies much lower in energy than either the bent/linear OUCCO structures or the U(CO)₂ uranium dicarbonyl.

Introduction

Reactions of uranium atoms with atmospheric components are of considerable interest due to the development of gas-phase separations involving atomic uranium. Mass spectrometric investigation and matrix isolation studies have focused on the oxidation of atomic uranium by molecular oxygen.^{1–4} Recent investigations of laser-ablated uranium atom reactions with O₂, N₂, and NO have characterized the inserted OUO, NUN, and NUO molecules in solid argon.^{4–6} Although reactions of solid uranium with carbon monoxide have been studied,^{7–9} little is known about reaction intermediates.

Stable transition-metal carbonyl complexes are prevalent; however, reports of actinide carbonyl complexes are remarkably scant. An earlier matrix infrared study of reaction of thermal uranium atoms with carbon monoxide has tentatively character-

ized uranium carbonyls ranging from UCO to U(CO)₆ in solid argon,¹⁰ and an investigation with laser-ablated uranium was complicated by the formation of uranium oxides.¹¹ In 1986, Andersen et al. isolated the first stable uranium carbonyl complex, (η^5 -Me₃SiC₅H₄)₃UCO.¹² This complex has a C–O stretching frequency of 1976 cm⁻¹, which suggests that U is a π -donor and theoretical corroboration for extensive U 5f → CO 2 π back-bonding has been presented.^{13,14} More recently, the complexes (η^5 -C₅Me₄H)₃UCO¹⁵ and (η^5 -C₅Me₅)₃UCO¹⁶ have been isolated, with solution C–O stretches at 1900 and 1925 cm⁻¹, respectively, which also suggest significant π back-bonding. We have previously reviewed the bonding and electronic structure in Cp–actinide complexes such as these Cp₃–UCO systems.¹⁷

Here we report a study of laser-ablated uranium atom reactions with carbon monoxide during condensation in excess neon. We will show that the CO-insertion product CUO, in addition to uranium carbonyls and their anions, is formed on

[†] University of Virginia.

[‡] The Ohio State University.

(1) Johnson, R.; Biondi, M. A. *J. Chem. Phys.* **1972**, *57*, 1975.

(2) Fite, W. L.; Lo, H. H.; Irving, P. J. *J. Chem. Phys.* **1974**, *60*, 1236.

(3) Lang, N. C.; Stern, R. C.; Finley, M. G. *Chem. Phys. Lett.* **1980**, *69*, 301.

(4) Hunt, R. D.; Andrews, L. *J. Chem. Phys.* **1993**, *98*, 3690.

(5) Hunt, R. D.; Yustein, J. T.; Andrews, L. *J. Chem. Phys.* **1993**, *98*,

6070. Kushto, G. P.; Souter, P. F.; Andrews, L. *J. Chem. Phys.* **1998**, *108*, 7121.

(6) Kushto, G. P.; Souter, P. F.; Andrews, L.; Neurock, M. *J. Chem. Phys.* **1997**, *106*, 5894.

(7) Stobbs, J. J.; Woodward, A. J. *J. Corros. Sci.* **1966**, *6*, 499.

(8) Whittle, I.; Gerrish, M. E.; Stobbs, J. J.; Buddery, J. H. *J. Less Common Met.* **1967**, *13*, 200.

(9) Paidassi, J.; Poinyud, M. L.; Caillat, R.; Darras, R. *J. Nucl. Mater.* **1961**, *3*, 161.

(10) Slater, J. L.; Sheline, R. K.; Lin, K. C.; Weltner, W., Jr. *J. Chem. Phys.* **1971**, *55*, 5129.

(11) Tague, T. J., Jr.; Andrews, L.; Hunt, R. D. *J. Phys. Chem.* **1993**, *97*, 10920.

(12) Brennan, J. G.; Andersen, R. A.; Robbins, J. L. *J. Am. Chem. Soc.* **1986**, *108*, 335.

(13) Bursten, B. E.; Strittmatter, R. J. *J. Am. Chem. Soc.* **1987**, *109*, 6606.

(14) Tatsumi, K.; Hoffmann, R. *Inorg. Chem.* **1984**, *23*, 1633.

(15) Parry, J.; Carmona, E.; Coles, S.; Hursthouse, M. *J. Am. Chem. Soc.* **1995**, *117*, 2649.

(16) Evans, W. J. Personal communication.

(17) Bursten, B. E.; Strittmatter, R. J. *Angew. Chem., Int. Ed. Engl.* **1991**, *30*, 1069.

deposition and on annealing. Photon-induced rearrangement of $\text{U}(\text{CO})_2$ to OUCCO and to $(\text{C}_2)\text{UO}_2$ molecules is also observed. Relativistic density functional calculations are used to corroborate the experimental findings and spectral assignments, and to predict the structures of the matrix-isolated species. The bonding and electronic structures of some of the key molecules discovered in this work will also be elucidated.

Experimental and Computational Section

The experiment for laser ablation and matrix isolation spectroscopy has been described in detail previously.^{18,19} Briefly, the Nd:YAG laser fundamental (1064 nm, 10 Hz repetition rate with 10 ns pulse width) was focused on the rotating metal uranium target (Oak Ridge National Laboratory) using low energy (1–5 mJ/pulse). Laser-ablated metal atoms were co-deposited with carbon monoxide (0.05–0.2%) in excess neon onto a 4 K CsI cryogenic window at 2–4 mmol/h for 30 min to 1 h. Carbon monoxide (Matheson) and isotopic $^{13}\text{C}^{16}\text{O}$ and $^{12}\text{C}^{18}\text{O}$ (Cambridge Isotopic Laboratories) and selected mixtures were used in different experiments. FTIR spectra were recorded at 0.5 cm^{-1} resolution on a Nicolet 750 spectrometer with 0.1 cm^{-1} accuracy using a HgCdTe detector. Matrix samples were annealed at different temperatures, and selected samples were subjected to broadband photolysis by a medium-pressure mercury arc (Philips, 175W, globe removed, 240–580 nm).

Relativistic density functional theoretical calculations have been performed by using the Amsterdam Density Functional (ADF 2.3) code,²⁰ with the inclusion of the generalized gradient approach of Perdew and Wang (PW91).²¹ The $[1s^2]$ cores for C and O and the $[1s^2-5d^{10}]$ core for U were frozen. Slater-type-orbital (STO) basis sets of triple- ζ quality were used for the valence orbitals of U, C, and O, with d- and f-type polarization functions for the C and O. Numerical integration accuracy of INTEGRATION=10.0 was used throughout.

The structures of calculated species were fully optimized with the inclusion of scalar (mass-velocity and Darwin) relativistic effects. When near-degenerate low-lying states were encountered, fractional occupation numbers were used to enforce the Aufbau principle. Vibrational frequencies were determined via numerical evaluation of the second-order derivatives of the total energies. Further computational details have been described elsewhere.²²

Results

Infrared spectra for the reaction of laser-ablated uranium with CO in excess neon reveal the strong absorptions for CO at 2140.7 cm^{-1} , CO^+ at 2194.3 cm^{-1} (not shown), $(\text{CO})_2^+$ at 2056.3 cm^{-1} , and $(\text{CO})_2^-$ at 1517.4 cm^{-1} (not shown),^{23,24} together with new product absorptions. The infrared spectra in the 2070–1640 and 1060–780 cm^{-1} regions with 0.1% CO in neon are illustrated in Figures 1 and 2, respectively, and the absorptions are listed in Table 1. The stepwise annealing and photolysis behavior of these product absorptions, also shown, will be discussed below. Different isotopic carbon monoxides $^{13}\text{C}^{16}\text{O}$ and $^{12}\text{C}^{18}\text{O}$ and the mixtures $^{12}\text{C}^{16}\text{O} + ^{13}\text{C}^{16}\text{O}$ and $^{12}\text{C}^{16}\text{O} + ^{12}\text{C}^{18}\text{O}$ were employed for product identification through isotopic shifts and splittings; the results using these

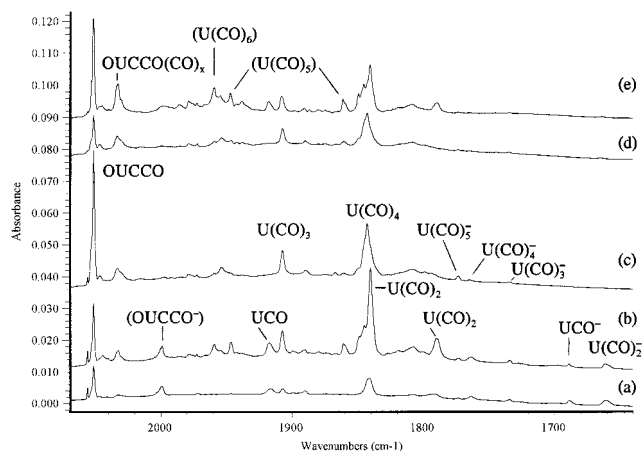


Figure 1. Infrared spectra in the 2070–1640 cm^{-1} region for laser-ablated U atoms co-deposited with 0.1% CO in neon: (a) after 30 min sample deposition at 4 K, (b) after annealing to 8 K, (c) after 15 min $\lambda > 290$ nm photolysis, (d) after 15 min full-arc photolysis, and (e) after annealing to 10 K.

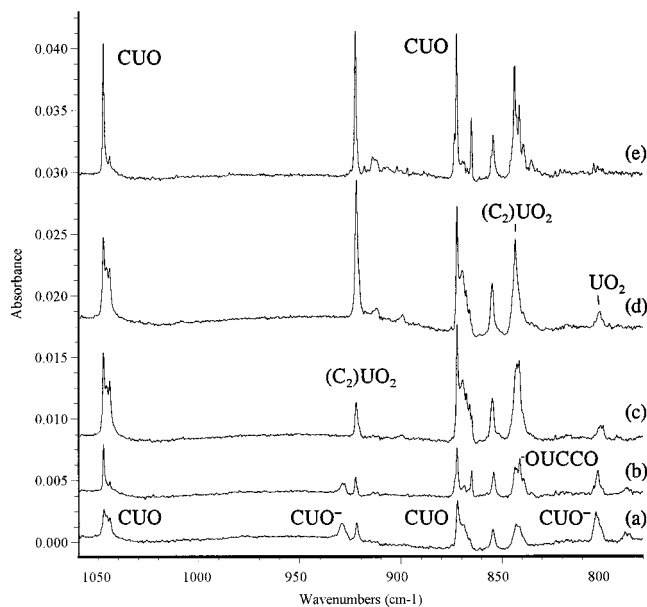


Figure 2. Infrared spectra in the 1060–780 cm^{-1} region for laser-ablated U atoms co-deposited with 0.1% CO in neon: (a) after 30 min sample deposition at 4 K, (b) after annealing to 8 K, (c) after 15 min $\lambda > 290$ nm photolysis, (d) after 15 min full-arc photolysis, and (e) after annealing to 10 K.

isotopic counterparts are also listed in Table 1. The mixed $^{12}\text{C}^{16}\text{O} + ^{13}\text{C}^{16}\text{O}$ spectra in the 2070–1740 and 1055–785 cm^{-1} regions are illustrated in Figures 3 and 4, respectively, and Figures 5 and 6 show the spectra in the 2060–1740 and 1055–750 cm^{-1} regions using a mixed $^{12}\text{C}^{16}\text{O} + ^{12}\text{C}^{18}\text{O}$ sample. Figure 7 contrasts isotopic mixtures in the 1300 cm^{-1} region. It is noteworthy that all of the product absorptions exhibit isotopic shifts, indicating reaction products with CO molecules. No UO and UO_2 absorption were observed in lower laser power experiments.

Discussion

The new reaction product molecules will be identified from infrared spectra of isotopic mixtures.

CUO. In previous argon matrix work, bands at 804.4 and 852.6 cm^{-1} were assigned to the CUO molecule. This assignment is incorrect; apparently trace oxygen impurity gave sufficient generation of UO_2 for the spectrum to be dominated

(18) Burkholder, T. R.; Andrews, L. *J. Chem. Phys.* **1991**, *95*, 8697.

(19) Hassanzadeh, P.; Andrews, L. *J. Phys. Chem.* **1992**, *96*, 9177.

(20) ADF 2.3, Theoretical Chemistry, Vrije Universiteit, Amsterdam.
(a) Baerends, E. J.; Ellis, D. E.; Ros, P. *Chem. Phys.* **1973**, *2*, 42. (b) te Velde, G.; Baerends, E. J. *J. Comput. Phys.* **1992**, *99*, 94. (c) Fonseca Guerra, C.; Visser, O.; Snijders, J. G.; te Velde, G.; Baerends, E. J. In *Methods and Techniques for Computational Chemistry*; Clementi, E., Corongiu, G., Eds.; STEF: Cagliari, 1995; p 305.

(21) (a) Perdew, J. P.; Wang, Y. *Phys. Rev. B* **1992**, *45*, 13244. (b) Perdew, J. P.; Chevary, J. A.; Vosko, S. H.; Jackson, K. A.; Pederson, M. R.; Singh, D. J.; Foilhais, C. *Phys. Rev. B* **1992**, *46*, 6671.

(22) Li, J.; Bursten, B. E. *J. Am. Chem. Soc.* **1997**, *119*, 9021.

(23) Thompson, W. E.; Jacox, M. E. *J. Chem. Phys.* **1991**, *95*, 735.

(24) Zhou, M. F.; Andrews, L. *J. Chem. Phys.* **1999**, *110*, 10370.

Table 1. Infrared Absorptions (cm^{-1}) Observed after Co-deposition of Laser-Ablated U Atoms with CO in Excess Neon at 4 K

$^{12}\text{C}^{16}\text{O}$	$^{13}\text{C}^{16}\text{O}$	$^{12}\text{C}^{18}\text{O}$	$^{12}\text{C}^{16}\text{O} + ^{12}\text{C}^{16}\text{O}$	$^{12}\text{C}^{16}\text{O} + ^{12}\text{C}^{16}\text{O}$	$R(^{12}\text{C}^{16}\text{O}/^{13}\text{C}^{16}\text{O})$	$R(^{12}\text{C}^{16}\text{O}/^{12}\text{C}^{18}\text{O})$	assignment
3395.0	3296.7	3349.8			1.0298	1.0135	OUCCO
2194.3							CO^+
2140.7	2093.6	2089.6	2140.7, 2093.6	2140.7, 2089.6	1.0225	1.0245	CO
2056.3	2010.9	2007.4	2067.4, 2056.3, 2018.4, 2010.9	2056.3, 2016.4, 2007.4	1.0226	1.0244	$(\text{CO})_2^+$
2051.5	1988.2	2030.5	2051.5, 2042.7, 1997.3, 1988.2	2051.5, 2030.5	1.0318	1.0103	OUCCO
2032.9	1972.7	2010.9	2032.7, 2026.0, 1980.9, 1973.2		1.0305	1.0109	OUCCO(CO) _x
1999.2	1933.4	1984.5		1999.2, 1984.5	1.0340	1.0074	(OUCCO) ⁻
1959.5	1917.6	1911.4			1.0219	1.0252	$(\text{U}(\text{CO})_6)^a$
1947.2	1904.8	1900.7			1.0224	1.0238	$(\text{U}(\text{CO})_5)^a$
1917.8	1875.5	1871.9	1917.7, 1875.4		1.0226	1.0245	$(\text{UCO})^a$
1907.4	1865.7	1863.1	1907.5, 1896.7, 1883.7, 1865.6	1907.4, 1896.3, 1882.4, 1863.1	1.0224	1.0238	$\text{U}(\text{CO})_3$
1890.1	1848.9	1843.8			1.0223	1.0251	?
1861.4	1820.9	1816.8			1.0222	1.0245	$(\text{U}(\text{CO})_5)$
1842.9	1802.8	1799.2	1946.5, 1937.3, 1926.3, 1843.0, 1802.8	1946.4, 1937.3, 1926.0, 1843.0, 1799.2	1.0222	1.0243	$\text{U}(\text{CO})_4$
1841.2	1801.4	1796.4			1.0221	1.0249	$\text{U}(\text{CO})_3$
1840.2	1801.1	1796.0	1840.3, 1827.4, 1800.7	1840.3, 1826.4, 1796.0	1.0217	1.0246	$\text{U}(\text{CO})_2$
1790.8	1752.1	1748.0	1790.6, 1764.5, 1752.0	1790.9, 1761.2, 1748.2	1.0221	1.0245	$\text{U}(\text{CO})_2$
1773.8	1734.8	1731.8			1.0225	1.0243	$(\text{U}(\text{CO})_5)^-a$
1764.4	1726.0	1722.6			1.0222	1.0242	$(\text{U}(\text{CO})_4)^-a$
1734.5	1696.1	1694.0			1.0226	1.0239	$(\text{U}(\text{CO})_3)^-a$
1689.2	1651.4	1650.3	1689.0, 1651.3		1.0229	1.0236	UCO^-
1661.2	1624.7	1620.5	1660.4, 1651.2, 1624.9		1.0225	1.0251	$\text{U}(\text{CO})_2^-$
1517.4	1484.2	1481.1	1517.4, 1499.4, 1484.2	1517.4, 1499.4, 1481.3	1.0224	1.0245	$(\text{CO})_2^-$
1516.4	1482.9	1480.3	1516.4, 1498.4, 1482.9	1516.3, 1498.4, 1480.3	1.0226	1.0244	$(\text{CO})_2^-$ site
1361.8	1324.9	1337.9	1361.7, 1359.6, 1327.6, 1324.9	1361.7, 1337.9	1.0279	1.0179	OUCCO
1360.3	1323.6	1336.4	1360.4, 1358.3, 1326.6, 1323.7		1.0277	1.0179	OUCCO site
1352.2	1315.5				1.0279		OUCCO(CO) _x
1047.3	1010.8	1046.3	1047.3, 1010.8	1047.3, 1046.2	1.0361	1.0010	CUO
1044.3	1007.9	1043.2	1044.3, 1007.9	1044.3, 1043.2	1.0361	1.0010	CUO site
929.3	896.8	928.5	929.1, 896.6		1.0362	1.0009	CUO^-
922.1	922.1	875.9		922.1, 905.2, 875.9		1.0527	$(\text{C}_2)\text{UO}_2$
872.2	870.5	826.4	872.2, 870.5	872.2, 826.5	1.0020	1.0554	CUO
864.9	863.1	819.8	865.1, 863.2	864.9, 819.7	1.0021	1.0550	CUO site
854.6	854.5	809.6		854.6, 809.6		1.0558	?
843.2	843.2	795.4		843.1, 812.8, 795.3		1.0601	$(\text{C}_2)\text{UO}_2$
841.0	841.0	796.2		841.0, 796.0		1.0563	OUCCO
838.9	838.9						OUCCO(CO) _x
803.3	801.6	761.1		803.3, 761.1	1.0021	1.0554	CUO^-

^a Parentheses denote tentative assignments.

by oxide complexes.⁴ The present study provides unequivocal evidence that CUO has vibrational bands at 1047.3 and 872.2 cm^{-1} in a neon matrix. These vibrational bands have similar profiles and are the dominant absorptions in the lower spectral region after sample deposition. The two bands tracked throughout all the experiments, both sharpened on 6 and 8 K annealing, both greatly increased in intensity on $\lambda > 290$ nm photolysis, and both sharpened more on 10 K annealing. All of these observations suggest that the 1047.3 and 872.2 cm^{-1} bands are due to different vibrational modes of the same molecule.

The 1047.3 cm^{-1} band shifted to 1010.8 cm^{-1} with $^{13}\text{C}^{16}\text{O}$, giving the $^{12}\text{C}^{16}\text{O}/^{13}\text{C}^{16}\text{O}$ isotopic frequency ratio 1.0361, which is slightly smaller than the calculated harmonic U–C value (1.0388) owing to some oxygen involvement (as noted by the 1.0 cm^{-1} shift with $^{12}\text{C}^{18}\text{O}$). On the other hand, the 872.2 cm^{-1} band shifted only 1.7 cm^{-1} with $^{13}\text{C}^{16}\text{O}$ and to 826.4 cm^{-1} with $^{12}\text{C}^{18}\text{O}$, giving a $^{12}\text{C}^{16}\text{O}/^{12}\text{C}^{18}\text{O}$ isotopic frequency ratio of 1.0554, which is also slightly lower than the harmonic U–O value (1.0565). The mixed $^{12}\text{C}^{16}\text{O} + ^{13}\text{C}^{16}\text{O}$ and $^{12}\text{C}^{16}\text{O} + ^{12}\text{C}^{18}\text{O}$ isotopic spectra (Figures 4 and 6) clearly indicate that only one C and one O atom are involved in each vibrational mode. Analogous to the NUO molecule,⁶ these two bands are assigned to the C–U and U–O stretching vibrations for the CUO molecule.

CUO is potentially a very interesting molecule. First, it is formally the result of the insertion of a uranium atom into the robust triple bond of CO and thus represents a new avenue for

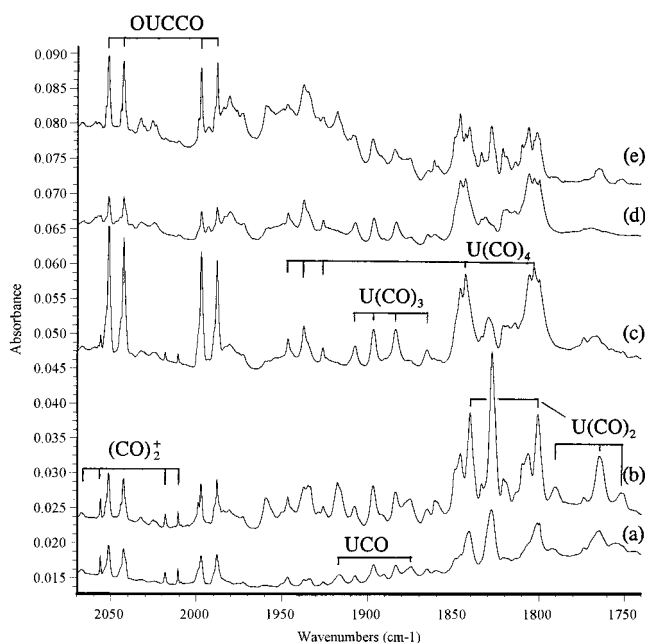


Figure 3. Infrared spectra in the 2070–1740 cm^{-1} region for laser-ablated U atoms co-deposited with 0.1% $^{12}\text{C}^{16}\text{O} + 0.1\%$ $^{13}\text{C}^{16}\text{O}$ in neon: (a) after 30 min sample deposition at 4 K, (b) after annealing to 8 K, (c) after 15 min $\lambda > 290$ nm photolysis, (d) after 15 min full-arc photolysis, and (e) after annealing to 10 K.

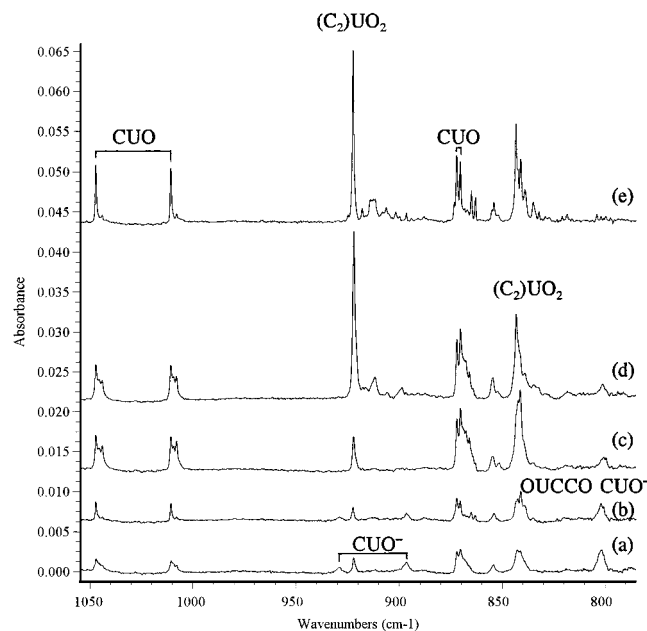


Figure 4. Infrared spectra in the 1055–785 cm^{-1} region for laser-ablated U atoms co-deposited with 0.1% $^{12}\text{C}^{16}\text{O}$ + 0.1% $^{13}\text{C}^{16}\text{O}$ in neon: (a) after 30 min sample deposition at 4 K, (b) after annealing to 8 K, (c) after 15 min $\lambda > 290$ nm photolysis, (d) after 15 min full-arc photolysis, and (e) after annealing to 10 K.

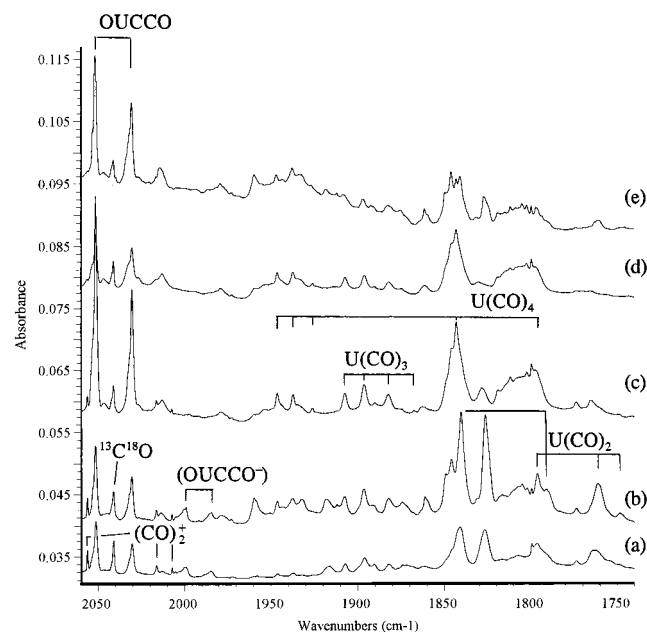


Figure 5. Infrared spectra in the 2060–1740 cm^{-1} region for laser-ablated U atoms co-deposited with 0.13% $^{12}\text{C}^{16}\text{O}$ + 0.07% $^{12}\text{C}^{18}\text{O}$ in neon: (a) after 30 min sample deposition at 4 K, (b) after annealing to 8 K, (c) after 15 min $\lambda > 290$ nm photolysis, (d) after 15 min full-arc photolysis, and (e) after annealing to 10 K.

the activation of small molecules. Second, it is a neutral molecule that is isoelectronic with the uranyl ion, UO_2^{2+} , which is certainly among the most studied of uranium-containing species.²⁵ The C–U bond in CUO might be expected to be more covalent than the O–U bond in UO_2^{2+} because of a more favorable match between the valence orbital energies of C and U.

The geometry and vibrational frequencies of CUO were recently addressed by Pyykkö and co-workers by using rela-

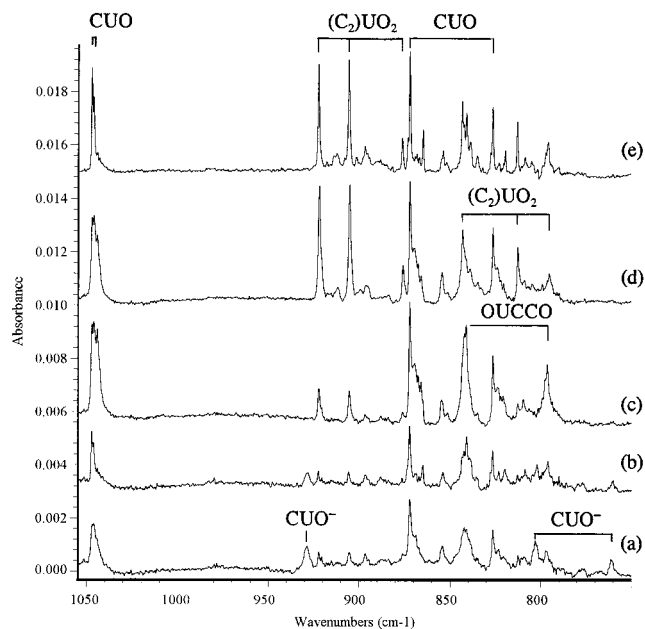


Figure 6. Infrared spectra in the 1055–750 cm^{-1} region for laser-ablated U atoms co-deposited with 0.13% $^{12}\text{C}^{16}\text{O}$ + 0.07% $^{12}\text{C}^{18}\text{O}$ in neon: (a) after 30 min sample deposition at 4 K, (b) after annealing to 8 K, (c) after 15 min $\lambda > 290$ nm photolysis, (d) after 15 min full-arc photolysis, and (e) after annealing to 10 K.

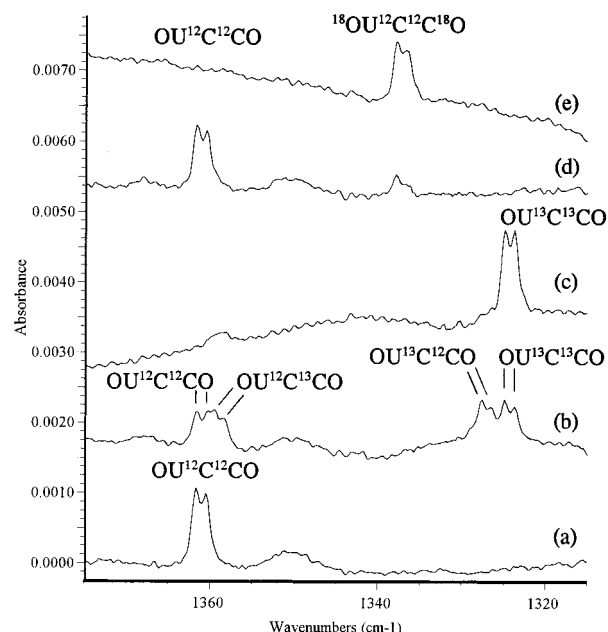


Figure 7. Infrared spectra in the 1375–1315 cm^{-1} region for laser-ablated U atoms co-deposited with isotopic CO in neon after $\lambda > 290$ nm photolysis: (a) 0.2% $^{12}\text{C}^{16}\text{O}$, (b) 0.1% $^{12}\text{C}^{16}\text{O}$ + 0.1% $^{13}\text{C}^{16}\text{O}$, (c) 0.2% $^{13}\text{C}^{16}\text{O}$, (d) 0.13% $^{12}\text{C}^{16}\text{O}$ + 0.07% $^{12}\text{C}^{18}\text{O}$, and (e) 0.2% $^{12}\text{C}^{18}\text{O}$.

tivistic Hartree–Fock pseudopotential calculations.²⁶ These calculations predict the C–U and U–O stretching modes at 1185 and 899 cm^{-1} for the linear CUO molecule. The calculated frequencies must be scaled by 0.884 and 0.970 to fit the observed values, which can be compared to the typical scale factor of 0.89 for RHF calculations of frequencies and to 0.87 for their calculation of the ν_3 mode of NUN with the same calculation.^{5,26} The higher energy mode was calculated to shift by 42 and 2 cm^{-1} with $^{13}\text{C}^{16}\text{O}$ and $^{12}\text{C}^{18}\text{O}$, respectively, while the lower mode was calculated to shift by 2 and 47 cm^{-1} with

(25) See for example: Denning, R. G. *Struct. Bonding* **1992**, 79, 215.

(26) Pyykkö, P.; Li, J.; Runeberg, N. *J. Phys. Chem.* **1994**, 98, 4809.

Table 2. Calculated Energies, Geometries, and Vibrational Properties of CUO and CUO⁻ ^a

	CUO			CUO ⁻		
	linear	bent	exptl	linear	bent	exptl
C–U	1.764	1.765		1.799	1.796	
U–O	1.808	1.810		1.840	1.846	
∠OUC	180	154.9		180	141.5	
<i>E</i>	-20.8299	-20.8244		-21.8419	-21.8500	
<i>ν</i> _b	63 (295)	59 (78)		87i (-14)	110 (65)	
<i>ν</i> _s (U–O)	877 (207)	881 (217)	872	821 (219)	822 (243)	803
<i>ν</i> _{as} (U–C)	1079 (158)	1071 (161)	1047	993 (180)	996 (206)	929

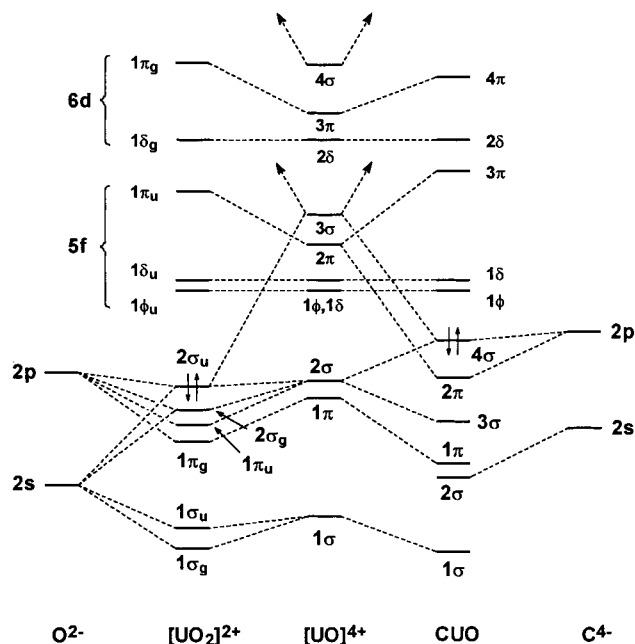
^a Bond lengths in Å, angles in deg, energies in eV, frequencies in cm⁻¹, and intensities (in parentheses) in km/mol.

¹³C¹⁶O and ¹²C¹⁸O, which are in very good agreement with our observed neon-matrix values.

To provide additional insight into the spectroscopic assignment of CUO and to provide a description of its bonding and a prediction of its structure, we have turned to relativistic density functional calculations. We will show that the present density functional calculations provide better agreement with the observed experimental results than do the Hartree–Fock results. Before addressing CUO, we performed benchmark calculations on the more symmetric isoelectronic molecule NUN, which has recently been detected in a frozen neon matrix at 1076.6 cm⁻¹.²⁷ On the basis of these calculations, we predict that NUN is linear (*D*_{∞h}) with a U–N distance of 1.73 Å, although the potential surface for bending of the molecule is very shallow. The calculated antisymmetric stretching frequency for linear NUN is 1099 cm⁻¹, which is in very good agreement with the observed frequency of 1076.6 cm⁻¹.

The UO₂²⁺ ion is linear or nearly so in all compounds that contain this moiety.²⁵ Nevertheless, the softness of the bending potential for NUN suggested to us that CUO might be a bent molecule; because of the asymmetry of the molecule, its vibrational spectroscopy could not unambiguously predict whether it is linear or bent. In our density functional calculations on CUO, therefore, we searched for minimum-energy structures in both linear (*C*_{∞v}) and bent (*C*_s) geometries. As shown in Table 2, the singlet CUO molecule is predicted to prefer slightly a linear structure, with U–C and U–O bond lengths of 1.764 and 1.808 Å, and vibrational frequencies of 1079, 877, and 63 cm⁻¹. A bent form of CUO (∠CUO = 154.9°), lying only 0.17 kcal/mol higher in energy than the linear one, possesses a slightly longer U–O bond length and similar frequencies. The ADF normal-mode analysis indicates that the antisymmetric (1079 cm⁻¹) and symmetric (877 cm⁻¹) bands correspond to the U–C and U–O stretching modes, respectively, which agrees well with the conclusions from the isotopic-substitution experiments. Note that the calculated frequencies are only slightly (3.0% and 0.6%) higher than the observed values, which provides further strong support for the identification of CUO.

Figure 8 provides a qualitative interaction diagram that compares the valence molecular orbitals of CUO to those of UO₂²⁺. We have constructed this diagram by allowing the MOs of the f⁰ fragment UO⁴⁺ to interact with the atomic orbitals of either O²⁻ or C⁴⁻. Only the 5f and 6d orbitals of U are shown, although the U 7s and 7p AOs contribute nonnegligibly to the bonding. The interaction of UO⁴⁺ with O²⁻ leads to the off-discussed and somewhat controversial²⁸ MOs of UO₂²⁺, which are labeled under *D*_{∞h} symmetry. The 2σ_u HOMO of UO₂²⁺

**Figure 8.** Qualitative interaction diagram showing the formation of the molecular orbitals of UO₂²⁺ and CUO by the interaction of O²⁻ and C⁴⁻ with UO⁴⁺.**Table 3.** Energies and Percent Compositions of the Occupied and Lowest Unoccupied Valence Molecular Orbitals of CUO

MO	<i>ε</i> _i (eV)	% contribution						
		U 6p	U 6d	U 5f	U 7s	U 7p	O	C
4π	-1.18		4	39		39	7	9
2δ	-2.09		85	14				
5σ	-3.12		14	4	50	5	8	18
1δ	-3.14		14	85				
1φ	-3.64			100				
4σ ^a	-4.02		13	42	12	3		28
2π	-4.89		21	31				47
3σ	-7.21	6	3	23	8		33	25
1π	-8.99		11	8			80	
2σ	-10.11		13	0	0	3	37	44
1σ	-19.76	25	2	1	0	3	53	17

^a Highest occupied molecular orbital (HOMO).

represents principally a strong covalent interaction between the O 2p_z AOs and the U 5f_{z³} AO. The occupied 2σ_g MO also largely involves the O 2p_z AOs, this time interacting with the U 6d_{z²} AO. These two MOs in particular effect a large transfer of electron density from the filled orbitals of O²⁻ into the empty orbitals of U⁶⁺. Our DFT calculations indicate that the percentage of U 5f and 6d contribution in the 2σ_u and 2σ_g MOs is 56% and 13%, respectively.

As expected, the bonding in CUO differs somewhat from that in UO₂²⁺ because of the higher energy of the C 2s and 2p orbitals relative to the O 2s and 2p AOs. Formally, the C–U and U–O bonds in CUO are triple bonds, as are the U–O bonds in UO₂²⁺. However, the degree of charge polarization is very different. In CUO, the atomic Mulliken charges are U(+1.36), C(-0.60), and O(-0.76), which is certainly in accord with electronegativity. These charges can be compared with U(+2.89) and O(-0.44) in UO₂²⁺. Because CUO has *C*_{∞v} symmetry, the U–O and U–C interactions can, in principle, localize and, because of the lack of inversion symmetry, can involve simultaneous contributions from the U 5f and 6d AOs. Indeed, these effects are observed, as is evident in the percent contributions of the MOs of CUO, listed in Table 3. For example, the 4σ HOMO of CUO is localized entirely between the U and C

(27) U + N₂, NO in neon: Zhou, M. F.; Andrews, L. *J. Chem. Phys.* **1999**, *111*, in press.

(28) See for example: Pepper, M.; Bursten, B. E. *Chem. Rev.* **1991**, *91*, 719.

atoms, and involves significant contributions from both the U $5f_{z^2}$ and U $6d_{z^2}$ AOs. The higher energy of the carbon AOs leads to an expected smaller HOMO-LUMO gap in CUO (0.4 eV) as compared to that in UO_2^{2+} (2.3 eV), which implies that CUO will have very different optical properties than UO_2^{2+} .

The better match in orbital energies in conjunction the greater diffuseness of the carbon AOs leads to a much more covalent interaction between C and U than between U and O. This effect is especially evident in the π -bonding MOs. The 1π MO ($E = -8.99$ eV) is a localized U–O π bond that is highly polarized: It is 80% O 2p in character, 11% U 6d, and 8% U 5f. By contrast, the 2π MO ($E = -4.89$ eV) is a localized, highly covalent π interaction between C and U: It is 47% C 2p, 21% U 6d, and 31% U 5f in character. We can view the mixing of the U 6d and 5f AOs in these MOs as the formation of “(d–f) π hybrids” that are directed at the O and the C orbitals. The greater covalency of the U–C interaction is what leads to the U–C bond being shorter than the U–O bond (1.764 vs 1.808 Å), even though the radius of O is smaller than that of C. The Mulliken overlap populations indicate that the U–C bond is more than two times stronger than the U–O bond in CUO. The calculated U–C and U–O force constants in CUO are consistent with this finding, as $F_{\text{UC}} = 8.27$ N/cm, $F_{\text{UO}} = 6.89$ N/cm, and $F_{\text{UC,UO}} = -0.05$ N/cm. By comparison, the calculated force constants in UO_2^{2+} are $F_{\text{UO}} = 9.96$ N/cm and $F_{\text{UO,UO}} = 0.27$ N/cm.

CUO⁻. Weak bands at 929.3 and 803.3 cm^{-1} were observed after deposition. They decreased in intensity together on annealing, were unchanged upon irradiation with $\lambda > 470$ nm, but disappeared upon $\lambda > 380$ nm photolysis (not shown). These two bands have isotopic shifts similar to the CUO molecular absorptions. The 929.3 cm^{-1} band shows a large (32.5 cm^{-1}) carbon isotopic shift and small (0.8 cm^{-1}) oxygen isotopic shift, while the 803.3 cm^{-1} band shows a small (1.7 cm^{-1}) carbon isotopic shift and large (42.2 cm^{-1}) oxygen shift. The mixed $^{12}\text{C}^{16}\text{O} + ^{13}\text{C}^{18}\text{O}$ and $^{12}\text{C}^{16}\text{O} + ^{12}\text{C}^{18}\text{O}$ isotopic spectra only give the sum of pure isotopic bands, and indicate single C and O atom involvement. These two bands are 118.0 and 68.9 cm^{-1} lower than the corresponding frequencies of CUO, and the photosensitive behavior and frequency reduction relative to CUO strongly suggest assignment to the CUO⁻ anion. The isoelectronic NUO molecule has been synthesized recently via reaction of laser-ablated uranium atoms with NO in excess neon,²⁷ and the 1004.9 and 833.5 cm^{-1} absorptions are slightly higher than the CUO⁻ bands in solid neon.

The density functional calculations for doublet CUO⁻ predict a bent molecular anion; constraining the anion to be linear leads to an imaginary frequency that indicates a saddle-point with respect to the bending coordinate of the molecule (Table 2). The predicted structure has U–O = 1.846 Å, U–C = 1.796 Å, and $\angle\text{C–U–O} = 141.5^\circ$. The calculated vibrational frequencies are 996, 822, and 110 cm^{-1} , which are in reasonable accord with the observed frequencies. In view of the agreement found for calculated frequencies for NUN and CUO, we believe that the agreement found for CUO⁻ strongly supports this assignment.

OUCCO. The present results also provide evidence for the reaction of two CO molecules with atomic U in the neon matrix. For example, three bands at 2051.5, 1361.8, and 841.0 cm^{-1} were observed after deposition, which increased together on 6 and 8 K annealing, markedly increased upon $\lambda > 290$ nm photolysis, decreased considerably upon full-arc photolysis, and almost recovered on 10 K annealing. The 2051.5 cm^{-1} band shifted to 1988.2 cm^{-1} with $^{13}\text{C}^{16}\text{O}$ and to 2030.5 cm^{-1} with

$^{12}\text{C}^{18}\text{O}$. These values give the 12/13 frequency ratio 1.0318 and 16/18 frequency ratio 1.0103, significantly larger and smaller than the ratios for diatomic CO, suggesting strong coupling with another C atom. In the mixed $^{12}\text{C}^{16}\text{O} + ^{13}\text{C}^{16}\text{O}$ experiment, a quartet with approximately 1:1:1:1 relative intensities was produced, while only pure isotopic counterparts were present in the mixed $^{12}\text{C}^{16}\text{O} + ^{12}\text{C}^{18}\text{O}$ experiment, indicating this is mainly a C–O stretching vibration coupled with one more inequivalent C atom. The 1361.8 cm^{-1} band has very similar behavior to the 2051.5 cm^{-1} band. The isotopic ratios (12/13: 1.0279, 16/18:1.0179) and mixed isotopic structures (Figure 7) also indicate the involvement of a CCO subunit. The 841.0 cm^{-1} band shows no carbon isotopic shift, but shifted to 796.2 cm^{-1} using $^{12}\text{C}^{18}\text{O}$; the isotopic 16/18 ratio of 1.0563 is very close to the diatomic UO ratio (1.0565), which indicates that this band is due to a terminal U–O stretching vibration. The doublet isotopic structure in mixed $^{12}\text{C}^{16}\text{O} + ^{12}\text{C}^{18}\text{O}$ spectra shows that only one O atom is involved in this mode. On the basis of these spectroscopic observations, these three bands are assigned to the OUCCO molecule.

A weak band at 3395.0 cm^{-1} showed the same annealing and photolysis behavior as the 2051.5, 1361.8, and 841.0 cm^{-1} bands. This band shifted to 3296.7 cm^{-1} with $^{13}\text{C}^{16}\text{O}$ and 3349.8 cm^{-1} with $^{12}\text{C}^{18}\text{O}$ giving the 12/13 frequency ratio 1.0298 and 16/18 frequency ratio 1.0135, which is near average values for the 2051.5 and 1361.8 cm^{-1} fundamental bands. The band position is just 18.3 cm^{-1} below the sum of 2051.5 and 1361.8 cm^{-1} bands. This band is assigned to the combination band of C–O stretching and C–CO stretching vibrations of the OUCCO molecule, and further corroborates the OUCCO assignment.

A weak band set at 2032.9, 1352.2, and 838.9 cm^{-1} shows isotopic shifts very similar to those of the OUCCO molecule. These bands increased together on higher temperature annealing while the OUCCO molecular absorptions decreased, and are tentatively assigned to the carbonyl adducts OUCCO·(CO)_n.

The assignments of the 2051.5, 1361.8, and 841.0 cm^{-1} bands to OUCCO are strongly supported by the density functional calculations (Table 4), which find a stable linear OUCCO molecule with strong stretching mode absorptions at 2125, 1393, and 897 cm^{-1} . These ADF calculated frequencies are again in excellent agreement (3.6, 2.3, and 6.7% high, respectively) with the observed values. Note that the U–O stretching mode (841.0 cm^{-1}) is more difficult to model theoretically than the C–C (1361.8 cm^{-1}) and C–O (2051.5 cm^{-1}) stretching modes, probably due to the neglect of spin–orbit coupling effects for the U atom. The ADF normal-mode analysis shows that the 2125 cm^{-1} band is the antisymmetric stretch of the triatomic CCO unit, which is a C–O stretch coupled with the neighboring C atom. The 1393 cm^{-1} band is predominantly the U–C stretch, coupled with the C–O stretch, whereas the 897 cm^{-1} band is a nearly pure U–O stretch. These theoretical analyses are completely consistent with the experimentally observed isotope effects on the frequencies. The OUCCO molecule is a triplet state with the $7s^1 5f^1$ configuration.

A weak band at 1999.2 cm^{-1} observed after deposition disappeared on $\lambda > 290$ nm photolysis and never recovered on higher temperature annealing. This band shifted to 1933.4 cm^{-1} with $^{13}\text{C}^{16}\text{O}$ and 1984.5 cm^{-1} with $^{12}\text{C}^{18}\text{O}$ giving the 12/13 ratio 1.0340 and 16/18 ratio 1.0074. In the mixed $^{12}\text{C}^{16}\text{O} + ^{12}\text{C}^{18}\text{O}$ experiment, a clear doublet was observed, while the mixed $^{12}\text{C}^{16}\text{O} + ^{13}\text{C}^{16}\text{O}$ product band was overlapped. This band is tentatively assigned to the C–O stretching vibration of the OUCCO⁻ anion. The C–CO and O–U stretching modes are probably much weaker and cannot be observed here. Doping

Table 4. Calculated Energies, Geometries, and Vibrational Properties of UC₂O₂ Isomers^a

<i>C_{∞v}</i> linear OUCCO, <i>E</i> = -38.2132 O-U = 1.795, U-C = 2.026, C-C = 1.298, C-O = 1.176 392 (51), 586 (21 × 2), 897 (326), 1393 (104), 2125 (1593)
<i>C_s</i> bent OUCCO, <i>E</i> = -38.0264 O-U = 1.819, U-C = 2.053, C-C = 1.302, C-O = 1.178 ∠OUC = 120.1, ∠UCC = 177.0, ∠CCO = 179.6 383 (70), 589 (28), 592 (32), 866 (245), 1363 (101), 2094 (1799)
<i>C_{2v}</i> planar (<i>η</i> ² -C ₂)UO ₂ , <i>E</i> = -39.3777 U-C = 2.278, U-O = 1.811, C-C = 1.276 ∠CUC = 32.5, ∠OUO = 132.5, ∠CUO = 97.5 328 (10), 498 (98), 855 (167), 876 (296), 1736 (0.1)
<i>C_{2v}</i> tetrahedral (<i>η</i> ² -C ₂)UO ₂ , <i>E</i> = -39.5911 U-C = 2.308, U-O = 1.794, C-C = 1.264 ∠CUC = 31.8, ∠OUO = 160.7, ∠CUO = 99.3 285 (18), 497 (101), 853 (66), 919 (361), 1802 (5)
<i>C₂</i> distorted tetrahedral (<i>η</i> ² -C ₂)UO ₂ , <i>E</i> = -39.6311 U-C = 2.289, U-O = 1.796, C-C = 1.271 ∠CUC = 32.2, ∠OUO = 155.8, ∠CUO = 92.5 327 (15), 492 (97), 849 (79, sym OUO), 910 (342, asym OUO), 1755 (1, C=C st)
<i>C_{2v}</i> U(CO) ₂ , <i>E</i> = -35.1938 U-C = 2.252, C-O = 1.174, ∠CUC = 76.2, ∠UCO = 179.4 318 (1), 335 (0.4), 343 (2), 1810 (778), 1861 (705)
<i>C_{2v}</i> U(CO) ₂ ⁻ , <i>E</i> = -36.4714 U-C = 2.215, C-O = 1.200, ∠CUC = 61.6, ∠UCO = 177.4 323 (20), 338 (3), 462 (5), 486 (21), 1665 (586), 1694 (1834)

^a Bond lengths in Å, angles in deg, energies in eV, frequencies in cm⁻¹, and intensities (in parentheses) in km/mol.

with 0.02% CCl₄ almost eliminated this band, which supports the anion identification. Although the CUO⁻ bands were masked by CCl₄ and one of its products, the absence of OUCCO⁻ suggests the absence of the CUO⁻ precursor.

(C₂)UO₂. The present experiments provide evidence for other products of the UC₂O₂ stoichiometry. The bands at 922.1 and 843.2 cm⁻¹ tracked together throughout all the experiments; these bands were weak after deposition, slightly decreased on annealing, but markedly increased on full-arc photolysis. Both bands exhibited no carbon isotopic shift with ¹³C¹⁶O, but shifted to 875.9 and 795.4 cm⁻¹ using ¹²C¹⁸O sample. The 16/18 ratios 1.0527 for the upper band and 1.0601 for the lower band are characteristic of antisymmetric and symmetric OUO vibrations. When a 2:1 mixture of ¹²C¹⁶O + ¹²C¹⁸O was used, both bands led to triplets with intensity ratios of approximately 4:4:1, indicating that two equivalent O atoms are involved in these two modes. Note the matching asymmetries in the triplet patterns: the middle component of the upper mode is 6.2 cm⁻¹ higher than the mean value of pure isotopic components, while the intermediate of the lower mode is 6.5 cm⁻¹ lower than the mean value, which further confirms assignment of the two bands to the same molecule. These two bands markedly increased in intensity upon photolysis while the OUCCO absorptions greatly decreased. These bands are assigned to the antisymmetric and symmetric OUO stretching vibrations of the (*η*²-C₂)UO₂ molecule, which is an isomer of OUCCO that is proposed to have a side-bound C-C fragment. The C-C stretching mode of the side-bound C₂ subunit is too weak to be observed here.

We used density functional calculations to explore the geometry of the proposed (*η*²-C₂)UO₂ molecule. The results are summarized in Table 4. Two limiting high-symmetry geometries were considered: a "planar" *C_{2v}* form in which all five atoms lie in the same plane, and a "tetrahedral" *C_{2v}* form in which the C-U-C plane is perpendicular to the O-U-O plane. Both of these forms led to a lower total energy than that in linear

OUCCO, presumably because of the formation of a second strong U-O bond; apparently the high oxophilicity of U favors the cleavage of a second molecule of CO by a single U atom. The tetrahedral form of (*η*²-C₂)UO₂ is ca. 0.21 eV lower in energy than the planar form, but both of these forms are only transition states based on the presence of a negative calculated frequency for the torsional mode corresponding to rotation of the C₂ fragment. A true minimum was obtained by relaxing the symmetry to C₂ point symmetry, corresponding to a twisting of the C₂ subunit about the 2-fold axis. The optimized structure has a dihedral angle of 55° between the C-U-C and O-U-O planes, i.e., it is closer to the tetrahedral limit than to the planar limit. The calculated bond lengths are U-C = 2.289 Å, U-O = 1.796 Å, and C-C = 1.271 Å, and the calculated O-U-O angle is 155.8°. The latter angle is near the O-U-O angle (161°) calculated²⁶ for UO₃, which can be viewed as (O)UO₂. The dihapto bonding in (*η*²-C₂)UO₂ is reminiscent of transition-metal peroxo complexes, (*η*²-O₂)MO₂.^{29,30}

The calculated frequencies at the optimized geometry of (*η*²-C₂)UO₂ provide excellent support for the proposed identification of this molecule. The antisymmetric and symmetric O-U-O modes are calculated at 910 and 849 cm⁻¹, respectively, just 12 and 6 cm⁻¹ from the observed values. Both of these modes are calculated to be intense, with the antisymmetric mode predicted to be the stronger, as expected. The C-C stretching mode is predicted at 1755 cm⁻¹, but it is calculated to be less than 1% as intense as the antisymmetric O-U-O stretch.

Although the calculated geometry of (*η*²-C₂)UO₂ is a twisted C₂ structure, the bonding in the molecule is more conveniently discussed in the higher symmetry tetrahedral *C_{2v}* geometry. The 922.1 cm⁻¹ antisymmetric OUO stretching mode in (*η*²-C₂)UO₂ is slightly higher than the 914.8 cm⁻¹ value for the linear OUO molecule recently observed in solid neon, but somewhat lower than the UO₂⁺ cation in solid neon at 980.1 cm⁻¹.³¹ For bonding analysis, the molecule can be viewed as the interaction of a closed-shell C₂²⁻ fragment ("doubly deprotonated acetylene") and a slightly bent closed-shell UO₂²⁺ fragment. The UO₂²⁺ fragment is formally f⁰d⁰ U(VI), so the interactions between C₂²⁻ and UO₂²⁺ are dominated by donations from the filled orbitals of the former into acceptor orbitals on the latter. In the coordinate system chosen, the U-O σ bonds of a bent UO₂²⁺ fragment are described by filled molecular orbitals of a₁ and b₁ symmetry. These bonding MOs are formed by donation from O-based electrons into primarily the empty 6d and 5f orbitals of the U atom.³² The corresponding a₁ and b₁ antibonding MOs are empty, are predominantly uranium-based, and are polarized away from the O atoms; these MOs are the primary acceptor orbitals for donation from a side-bound C₂ fragment. The principal donor orbitals of C₂²⁻ are the filled π MOs. One of these will lie in the C-U-C plane (π_{||}) and the other is perpendicular to the C-U-C plane (π_⊥).

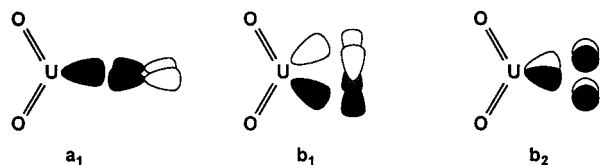
The dominant interactions between C₂²⁻ and UO₂²⁺ are shown pictorially in Scheme 1. The empty a₁ orbital of UO₂²⁺ is primarily a hybrid of the U 6d_{z²}, 5f_{z³}, and 7s orbitals that is directed away from the O atoms. It can interact with the π_{||} MO of C₂²⁻ regardless of the rotational orientation of the C₂²⁻ subunit. This interaction imparts no rotational preference to the bonding of C₂²⁻ to UO₂²⁺. The empty b₁ orbital of UO₂²⁺ is a

(29) Zhou, M. F.; Andrews, L. *J. Phys. Chem. A* **1998**, *102*, 8251.

(30) Citra, A.; Andrews, L. *J. Phys. Chem. A* **1999**, *103*, 4182.

(31) UO₂ in solid neon, 914.8 cm⁻¹; UO₂⁺ in solid neon, 980.1 cm⁻¹; Zhou, M. F.; Andrews, L. Unpublished.

(32) In linear UO₂²⁺, the a₁ and b₁ MOs become σ_g⁺ and σ_u⁺ MOs, respectively. By symmetry, the former can involve U 6d and 7s atomic orbitals whereas the latter can involve U 5f and 7p AOs.

Scheme 1. Principal Orbital Interactions between C_2^{2-} and UO_2^{2+} 

mixture of mainly the $U 5f_{x(x^2-3y^2)}$, $5f_{xz^2}$, and $6d_{xz}$ that is polarized away from the O atoms. It can interact with the π_{\perp} MO of C_2^{2-} in the “tetrahedral” C_{2v} geometry of $(\eta^2-C_2)UO_2$. It is this interaction that favors the tetrahedral C_{2v} geometry over the planar C_{2v} geometry for the molecule. There is also an acceptor orbital of b_2 symmetry that is the antibonding counterpart of one of the U–O π bonding MOs. This b_2 MO is oriented in the plane perpendicular to the plane of the UO_2 fragment and is not as strongly polarized toward the C_2 subunit as is the b_1 MO. It can interact with the π_{\perp} MO of C_2^{2-} in the planar C_{2v} geometry of $(\eta^2-C_2)UO_2$. The calculated C_2 structure of $(\eta^2-C_2)UO_2$ is the result of a compromise between these b_1 and b_2 interactions, the b_1 being somewhat stronger than the b_2 and thus favoring a geometry closer to the tetrahedral C_{2v} limit. Population analysis indicates that the C_2^{2-} fragment transfers about 1.5e to the UO_2^{2+} fragment. The atomic charges in $(\eta^2-C_2)UO_2$ are U(+1.87), O(−0.70), and C(−0.24), which compares to U(+2.89) and O(−0.44) in linear UO_2^{2+} . The donation from the filled π orbitals of C_2^{2-} decreases the bond order in that fragment from its idealized value of three; consistent with that notion, the calculated C–C bond length in $(\eta^2-C_2)UO_2$ is 1.27 Å, which is intermediate between a typical C–C triple bond and a C–C double bond. This may be compared with the HF/6-31G* computed bond length (1.26 Å) for the free dicarbide (C_2^{2-}) anion.³³ The donation of electron density into formally U–O antibonding MOs of UO_2^{2+} also serves to weaken and therefore lengthen the U–O bonds in $(\eta^2-C_2)UO_2$ (calculated U–O = 1.796 Å) relative to those of UO_2^{2+} (calculated U–O = 1.713 Å). The weakening of the U–O bonds also leads to a large red-shift of the predominantly U–O stretching modes of $(\eta^2-C_2)UO_2$ (calculated: $\nu_{\text{sym}} = 849 \text{ cm}^{-1}$, $\nu_{\text{asym}} = 910 \text{ cm}^{-1}$) relative to those of linear UO_2^{2+} (calculated: $\nu_{\text{sym}} = 993 \text{ cm}^{-1}$, $\nu_{\text{asym}} = 1092 \text{ cm}^{-1}$). As based on Mulliken overlap populations, the U–O bond in the bent “uranyl” of $(\eta^2-C_2)UO_2$ has been weakened by ca. 20% when compared with the U–O bond in the linear uranyl UO_2^{2+} .

$U(CO)_x$ ($x = 1-6$). Several of the bands observed upon co-deposition of U and CO in neon are in the frequency range expected for metal carbonyl complexes. A weak band at 1917.8 cm^{-1} increased on annealing, and was favored in lower CO concentration experiments. The isotopic 12/13 ratio 1.0226 and 16/18 ratio 1.0245 are characteristic of carbonyl stretching vibrational ratios. In both mixed isotopic experiments, only pure isotopic counterparts were observed, but the region is congested and this band is tentatively assigned to the uranium monocarbonyl UCO molecule. Both previous U/CO studies reported an 1893 cm^{-1} band in the initial argon matrix, but neither assigned this band to UCO.^{10,11} The present neon matrix experiments suggest reassignment of this band to the UCO species.

The observation of three cyclopentadienyl-substituted uranium carbonyl complexes with C–O frequencies in the 1976–1900 cm^{-1} range are in accord with the 1917.8 cm^{-1} band for neon matrix-isolated UCO.^{12,15,16} Unfortunately, density functional calculations provide relatively poor results in the case of UCO.

The calculations find that the averaged quintet ($2S + 1 = 5$) state, corresponding to $U 7s^2 6d^1 5f^3$ atomic configuration, has a lower energy than those of the singlet, triplet, and septet states. Quintet UCO is predicted to have a linear structure with a C–O stretch at 1818 cm^{-1} , which is 100 cm^{-1} (5%) lower than the experimental frequency. This rather large discrepancy can be attributed in part to the near-generacy effect arising from the multiple spatial configurations.

The bands at 1840.2 and 1790.8 cm^{-1} increased together on annealing and disappeared on photolysis. The isotopic frequency ratios for these bands are listed in Table 1. In both mixed isotopic experiments, triplets were observed for each band, indicating that two equivalent CO units are involved. These two bands are assigned to the symmetric and antisymmetric C–O stretching vibrations, respectively, of the bent $U(CO)_2$ molecule. The symmetric stretching vibration is more intense than the antisymmetric vibration, suggesting that the C–U–C angle is $\leq 90^\circ$. The $U(CO)_2$ assignment is nicely supported by the density functional calculations, which predict a septet ground state for the molecule with C_{2v} symmetry and a $\angle CUC$ bond angle of 76.2°. The antisymmetric and symmetric C–O stretching modes are calculated to occur at 1861 and 1810 cm^{-1} , respectively, with the later being 10% more intense.

The 1907.4 cm^{-1} band was also weak after deposition and increased markedly on annealing. In mixed $^{12}C^{16}O + ^{12}C^{18}O$ experiments, a quartet was produced at 1907.5, 1896.7, 1883.7, and 1865.6 cm^{-1} with approximately 1:3:3:1 relative intensities, which is characteristic of the nondegenerate mode of trigonal species. Similar mixed isotopic structure was observed in mixed $^{12}C^{16}O + ^{12}C^{18}O$ spectra as shown in Figure 3. This band is assigned to the symmetric C–O stretching vibration of the $U(CO)_3$ molecule with C_{3v} symmetry. The antisymmetric stretching vibration is mostly likely observed at 1841.2 cm^{-1} but is partly overlapped with other carbonyl absorptions.

The 1842.9 cm^{-1} band was only observed on annealing and markedly increased on photolysis. This band shifted to 1802.8 cm^{-1} with $^{13}C^{16}O$ and 1799.2 cm^{-1} with $^{12}C^{18}O$ giving the 12/13 ratio 1.0222 and 16/18 ratio 1.0243. In mixed $^{12}C^{16}O + ^{13}C^{16}O$ spectra, strong pure isotopic counterparts were observed together with three extra higher bands at 1946.5, 1937.3, and 1926.3 cm^{-1} . The 1946.5, 1937.3, and 1926.3 cm^{-1} bands have approximately 1:2:1 relative intensities. This isotopic structure is characteristic of a tetrahedral $U(CO)_4$ molecule.³⁴ The intermediates of the triply degenerate C–O stretching vibration are weaker, and cannot be resolved here due to band overlap, while the nondegenerate stretching vibration of partly isotopic substituted molecules gains intensity via symmetry lowering and coupling with the antisymmetric stretching vibration. The same mixed isotopic structure was observed in mixed $^{12}C^{16}O + ^{12}C^{18}O$ spectra, but in this case, the $^{12}C^{16}O$ enrichment is twice that of the $^{12}C^{18}O$ sample, and gave approximately 4:4:1 relative intensities for the symmetric stretching vibration of the partly substituted molecule.

The $U(CO)_5$ and $U(CO)_6$ assignments are not straightforward. The 1947.1 cm^{-1} band was produced on annealing, decreased on photolysis, and increased on higher temperature annealing. A band at 1861.4 cm^{-1} seems to track with a 1947.1 cm^{-1} band, and both bands show carbonyl stretching vibrational ratios. These two bands are tentatively assigned to the $U(CO)_5$ molecule. The 1959.5 cm^{-1} band, also produced on annealing, increased greatly on higher temperature annealing. In mixed

(33) Pyykkö, P.; Zhao, Y.-F. *J. Phys. Chem.* **1990**, *94*, 7753.(34) Darling, J. H.; Ogden, J. S. *J. Chem. Soc., Dalton Trans.* **1972**, 2496.

experiments, no obvious intermediate components were observed, and this band is tentatively assigned to the $\text{U}(\text{CO})_6$ molecule.

Our assignments are in disagreement with earlier argon matrix work, which tentatively assigned two bands at 1817, 1832 cm^{-1} to the monocarbonyl, 1846 and 1855 cm^{-1} to the dicarbonyl, and 1893, 1919, 1938, and 1961 cm^{-1} to the $\text{U}(\text{CO})_{3-6}$ molecules.¹⁰ As can be seen in their Figure 1, the 1893 cm^{-1} band, which was assigned to $\text{U}(\text{CO})_3$, is the only absorption in this region present after deposition. This band is the best candidate for the UCO molecule, which is in good agreement with our 1917.8 cm^{-1} neon matrix value. The 1846 and 1855 cm^{-1} argon matrix bands are too high for the dicarbonyl compared to the 1790.8 and 1840.2 cm^{-1} neon matrix values. However, the $\text{U}(\text{CO})_5$ and $\text{U}(\text{CO})_6$ bands are close to our neon matrix values, which were the dominant absorptions after higher temperature annealing.

$\text{U}(\text{CO})_x^-$ ($x = 1-5$). Weak bands in the 1780–1650 cm^{-1} region are photosensitive, a behavior analogous to anionic species recently reported in experiments with first row transition metal elements.³⁴⁻³⁶ Further, doping with CCl_4 reduced these bands to less than 10% of their absorbance in Figure 1. The 1689.2 cm^{-1} band decreased on annealing and disappeared on $\lambda > 380$ nm photolysis, and no intermediates were observed on both mixed $^{12}\text{C}^{16}\text{O} + ^{13}\text{C}^{16}\text{O}$ and $^{12}\text{C}^{16}\text{O} + ^{12}\text{C}^{18}\text{O}$ experiments. The 1689.2 cm^{-1} band is assigned to the UCO^- anion. In contrast to UCO, the density functional calculations provide excellent support for this assignment. The UCO^- anion is calculated to be linear with a sextet ground state. The calculated C–O stretching frequency is 1694 cm^{-1} , which is only 5 cm^{-1} higher than the experimental value.

The broad 1661.2 cm^{-1} band also decreased on annealing and disappeared on $\lambda > 380$ nm photolysis. In the mixed $^{12}\text{C}^{16}\text{O} + ^{13}\text{C}^{16}\text{O}$ experiment, a triplet is observed, consistent with the $\text{U}(\text{CO})_2^-$ anion. The mixed-isotope counterpart is blue-shifted relative to the mean value of the pure isotopic components, suggesting that the 1661.2 cm^{-1} band is due to the symmetric C–O stretch; as mentioned above, the symmetric stretch in $\text{U}(\text{CO})_2$ is more intense than the antisymmetric stretch. The weaker antisymmetric stretch for $\text{U}(\text{CO})_2^-$ is probably obscured by other absorptions in the water region. Our density functional calculations lead to the prediction that $\text{U}(\text{CO})_2^-$ should have a sextet ground state. The antisymmetric and symmetric C–O stretches are predicted to occur at 1665 and 1694 cm^{-1} , with the infrared intensity of the latter about 3 times greater than that of the former. These results provide strong support for the experimental assignment for the $\text{U}(\text{CO})_2^-$ anion.

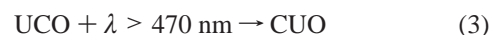
There are three bands at 1734.5, 1764.4, and 1773.8 cm^{-1} which show carbonyl stretching vibrational ratios. The 1734.5 and 1764.4 cm^{-1} bands almost disappeared on $\lambda > 290$ nm photolysis, while the 1773.8 cm^{-1} band was only eliminated on more energetic full-arc photolysis. According to recent matrix photochemistry of first-row transition-metal carbonyl anions,³⁵⁻³⁷ the energy required to photobleach $\text{M}(\text{CO})_x^-$ anions increases as x increases. Hence, by analogy, we tentatively assign the 1734.5 cm^{-1} band to $\text{U}(\text{CO})_3^-$, the 1764.4 cm^{-1} band to $\text{U}(\text{CO})_4^-$, and the 1773.8 cm^{-1} band to $\text{U}(\text{CO})_5^-$.

Reaction Mechanisms. Laser-ablated uranium atoms co-deposited with CO molecules in excess neon produced uranium carbonyls as well as the CUO insertion product. The uranium carbonyls increased on annealing, suggesting that reactions 1

is exothermic with minimal activation energy. The CUO molecules must be formed by insertion reaction 2; the CUO absorption slightly decreased on



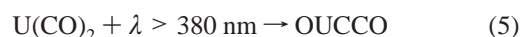
annealing and greatly increased on photolysis, indicating that reaction 2 requires some activation energy, analogous to the $\text{U} + \text{N}_2$ reaction.⁵ There is no UO detected in our experiments, suggesting that the insertion reaction product CUO is stable to dissociation. The UCO absorption decreased on $\lambda > 470$ nm photolysis and disappeared on $\lambda > 290$ nm photolysis, which is consistent with the isomerization of UCO to CUO proposed in reaction 3.



The absorptions due to the OUCCO molecule increased on annealing, which indicates that OUCCO can be formed by the simple addition reaction 4. Further, the bands for OUCCO

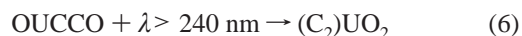


increased on photolysis with $\lambda > 380$ nm (and markedly with $\lambda > 290$ nm), during which the absorptions of $\text{U}(\text{CO})_2$ disappeared. These observations suggest that $\text{U}(\text{CO})_2$ undergoes photoinduced isomerism to OUCCO, as shown in reaction 5.



The absorptions due to the higher uranium carbonyl complexes also decreased on photolysis, during which the amount of $(\text{CO})_x\text{OUCCO}$ increased. It appears that near-ultraviolet light initiates insertion reaction 5 for higher carbonyl complexes. The density functional calculations suggest that the linear OUCCO molecule is more stable than the bent $\text{U}(\text{CO})_2$ dicarbonyl isomer by about 70 kcal/mol. By comparison, in the case of Zr, Hf, and Ta, the OMCCO isomers are calculated to be about 33–48 kcal/mol lower in energy than the $\text{M}(\text{CO})_2$ dicarbonyl species using density functional theory and pseudopotentials.³⁸

On full-arc photolysis, $(\eta^2\text{-C}_2)\text{UO}_2$ is produced at the expense of OUCCO, suggesting the photoinduced isomerism in reaction 6. Our density functional calculations find $(\eta^2\text{-C}_2)\text{UO}_2$ to be 102 kcal/mol more stable than $\text{U}(\text{CO})_2$. It is interesting to note that higher energy UV excitation is required to initiate rearrangement reaction 6 than reaction 5.



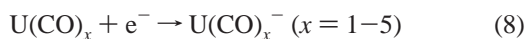
Laser ablation produces not only neutral metal atoms but also metal cations and electrons. As a result, molecular anions can be formed via electron capture by neutral molecules and molecular cations can be produced by metal cation reactions or ionization processes. In addition to the neutral molecules discussed above, the present experiments also led to the formation of the $\text{U}(\text{CO})_x^-$ and CUO^- anions along with the common CO^+ , $(\text{CO})_2^+$, cations and $(\text{CO})_2^-$ anion.^{23,24} The $\text{U}(\text{CO})_x^-$ and CUO^- anions are presumably formed by the electron capture of neutral molecules, as proposed in reactions 7 and 8.

(38) Ta + CO: Zhou, M. F.; Andrews, L. *J. Phys. Chem. A* In press.

(35) Zhou, M. F.; Andrews, L. *J. Am. Chem. Soc.* **1998**, *120*, 11499.

(36) Zhou, M. F.; Chertihin, G. V.; Andrews, L. *J. Chem. Phys.* **1998**, *109*, 10893.

(37) Zhou, M. F.; Andrews, L. *J. Phys. Chem. A* **1998**, *102*, 10250.



Conclusions

Laser-ablated uranium atoms react with CO molecules during condensation in excess neon. On the basis of isotopic substitution, absorptions at 1047.3 and 872.2 cm^{-1} are assigned to U–C and U–O stretching vibrations of the insertion product CUO, a reaction that requires activation energy. This measurement clearly identifies the U–C vibrational frequency. The calculated U–C bond length in CUO is the shortest and strongest U–C bond yet characterized (calculated 1.764 Å), much shorter than that found (2.29 Å) for $[\text{Cp}_3\text{UCH}\{\text{P}(\text{CH})_3\}_2(\text{C}_6\text{H}_5)]$.³⁹

Absorptions at 2051.5, 1361.8, and 841.0 cm^{-1} are assigned to the OUCCO molecule, which is formed by CO addition to CUO and by ultraviolet–visible photoinduced isomerism of the U(CO)_2 molecule. The OUCCO molecule undergoes further photoinduced rearrangement to the $(\eta^2\text{-C}_2)\text{UO}_2$ molecule, which

(39) Cramer, R. E.; Maynard, R. B.; Paw, J. C.; Gilje, J. W. *J. Am. Chem. Soc.* **1981**, *103*, 3589.

is characterized by symmetric and antisymmetric OUO vibrations at 843.2 and 922.1 cm^{-1} .

The uranium carbonyls U(CO)_x ($x = 1-6$) are formed on deposition or on annealing. The carbonyl stretching frequency observed here for UCO, 1917 cm^{-1} , is in the same range as the 1976 cm^{-1} vibration observed for the first stable uranium carbonyl complex, $(\text{Me}_3\text{SiC}_5\text{H}_4)_3\text{UCO}$, and the 1900 cm^{-1} vibration exhibited by $(\text{C}_5\text{Me}_4\text{H})_3\text{UCO}$.^{12,15} Evidence is also presented for the CUO^- anion and U(CO)_x^- ($x = 1-5$) anions, which are formed by electron capture of the neutral molecules.

Acknowledgment. We gratefully acknowledge N.S.F. support for this research from the National Science Foundation (Grant CHE 97-00116 to L.A.), from the Division of Chemical Sciences, U.S. Department of Energy (Grant DE-FG02-86ER13529 to B.E.B.), and from the Ohio Supercomputer Center and the Environmental Molecular Sciences Laboratory at Pacific Northwest National Laboratory for grants of computer time. Preliminary ADF calculations were performed by S. P. Willson with the assistance of M. Neurock at Virginia.

JA9921322